Frequency Selection for Accurate Radar System of 2D Airplane in Turbulence Using Beam Wave Incidence

Hosam El-Ocla

Department of Computer Science
Lakehead University, 955 Oliver Road, Thunder Bay, Ontario, Canada P7B 5E1
hosam.elocla@lakeheadu.ca

Abstract **–** Selection of the proper frequencies that are able to detect civil and military aircrafts is a challenging issue in radar engineering. Proposed algorithm measures the effect of the linear polarization including H-wave polarization on the radar detection behavior in random medium, and hence, compares it with the E-wave polarization case. Effects of random medium properties on the scattered waves are analyzed. In doing this, laser radar cross section (LRCS) of targets is calculated using a boundary value method with a beam wave incidence. As a result, performance of the backscattering enhancement is studied with the object configuration considering the creeping waves that have an obvious impact, particularly in the resonance region.

Index Terms **–** Airplane, beam, conducting, frequency, object, polarization, scattering, radar, turbulence.

I. INTODUCTION

Recently, plenty of researchers presented useful quantitative studies for a range of frequencies able to detect a variety of conducting objects such as aircrafts and ships [1-3]. The case where targets are embedded in random media produces a backscattering enhancement in electromagnetic waves [4-6] compared to the free space case. Accordingly, the double passage effect [4] is applied on waves backscattering from point targets where RCS is enhanced by a factor ranging from one to two (Rayleigh) to three, because of the correlation between the forward and backward fields in turbulence [6].

In [7], it was handled the problem of backscattering enhancement where authors discussed the importance of using a boundary value problem method to calculate the generated surface current, essentially the effect of the shadow region when the object dimensions are larger than the wavelength λ. Over the past years, a current generator method (CGM) has been presented to solve the scattering problem as a boundary value problem [8,9]. This method computes reflected waves from the whole surface of arbitrary shape objects with reasonable processing time. Actually, our results are in excellent agreement with those assuming a cylinder with circular cross section in free space in [10]. Recently, CGM was verified using FDFD method and proved a fair agreement with an accuracy below 5% error rate for objects in random media and even less error in the free space [11]. In [12], it was concluded that RCS and accordingly the backscattering enhancement for a plane wave incidence depends greatly on the incident angle and the configuration of the target regardless of the incident wave polarization. However, this is not the case with E-beam wave incidence, particularly in the range of $a \geq \lambda$ [13].

In this paper, we extend our work to investigate the effect of beam wave incidence assuming H-polarization on objects having different configurations. With H-polarization, creeping waves [14] are generated and their effect maximizes in the resonance region where the target size is close to λ [15]. To improve radar imaging in the sense of having an accurate RCS calculation of objects such as aircrafts in turbulence, resonance effect [16] should be avoided or at least minimized to its minimal by controlling the incident aspects as it is investigated here. This is to obtain a radar system almost independent of the incident angle and complexity of aircrafts shapes. Therefore, the range of frequencies to detect accurately civil and military airplanes is selected despite of the coherence function of the surrounding medium, the incident wave polarization, and the illumination region complexity for some canonical examples. The time factor exp(−iwt) is assumed and suppressed in the following section.

II. SCATTERING PROBLEM

Geometry of the problem is shown in Fig. 1. A random medium is assumed as a sphere of radius L around a target of the mean size $a \ll L$, and also to be described by the dielectric constant ε(r), the magnetic permeability μ, and the electric conductivity σ. For simplicity ε(r) is expressed as:

$$\varepsilon(\mathbf{r}) = \varepsilon_0[1+\Delta\varepsilon(\mathbf{r})], \quad (1)$$

Submitted On: December 14, 2014
Accepted On: June 6, 2015

where ε_0 is assumed to be constant and equal to the permittivity of free space and $\Delta\varepsilon(\mathbf{r})$ is a random function with:

$$\langle\Delta\varepsilon(\mathbf{r})\rangle = 0, \qquad \langle\Delta\varepsilon(\mathbf{r})\,\Delta\varepsilon(\mathbf{r}')\rangle = B(\mathbf{r},\mathbf{r}'), \tag{2}$$

and

$$B(\mathbf{r},\mathbf{r}'),\ll 1, \qquad kl(\mathbf{r}) \gg 1. \tag{3}$$

Here, the angular brackets denote the ensemble average and $B(\mathbf{r},\mathbf{r}')$, $l(\mathbf{r})$ are the local intensity and local scale-size of the random medium fluctuation, respectively, and $k = \omega\sqrt{\varepsilon_0\mu_0}$ is the wavenumber in free space. Also μ and σ are assumed to be constants; $\mu = \mu_0$, $\sigma = 0$. For practical turbulent media the condition (3) may be satisfied. Therefore, we can assume the forward scattering approximation and the scalar approximation [15].

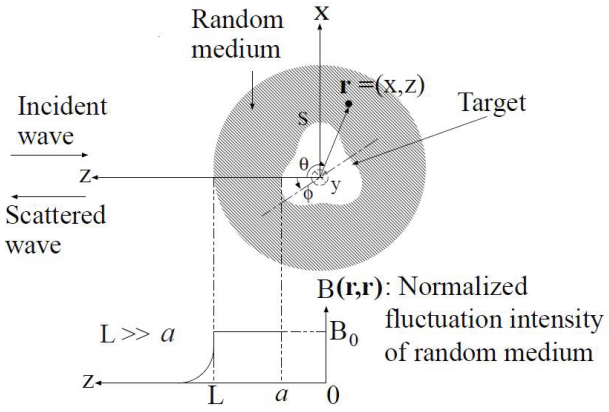

Fig. 1. Problem description of wave scattering from a conducting cylinder in random medium.

Consider the case where a directly incident wave is produced by a line source $f(\mathbf{r}')$ distributed uniformly along the y-axis. The line source is located at r_t beyond the random medium and it is quite far from the target. An electromagnetic wave radiated from the source propagates in the random medium illuminating the target and induces a current on its surface. A scattered wave from the target is produced by the surface current and propagates back to the observation point that coincides with the source point. The target is assumed to be a conducting cylinder of which cross-section is expressed by:

$$r = a\left[1-\delta\cos 3\left(\theta-\phi\right)\right], \tag{4}$$

where ϕ is the rotation index, δ is the concavity index. We can deal with this scattering problem two dimensionally under the condition (3); therefore, we represent $\mathbf{r}$ as $\mathbf{r} = (x, z)$. Assuming an H-polarization of incident waves (H-wave incidence), we can impose the Neumann boundary condition for wave field $u(\mathbf{r})$ on the cylinder surface S. That is,

$$\frac{\partial}{\partial n}u(\boldsymbol{r}) = 0, \tag{5}$$

where $u(\mathbf{r})$ represents E_x. Here, let us designate the incident wave by $u_{in}(\mathbf{r})$, the scattered wave by $u_s(\mathbf{r})$, and the total wave by $u(\mathbf{r}) = u_{in}(\mathbf{r}) + u_s(\mathbf{r})$. According to the current generator method [9] that uses the current generator Y_H and the Green's function in random medium $G(\mathbf{r}|\mathbf{r}')$ and as in [12], we can express the surface current wave as:

$$u(\boldsymbol{r_2}) = J_H(\boldsymbol{r_2}) = -\int_S Y_H(\boldsymbol{r_2}|\boldsymbol{r_1})\,u_{in}(\boldsymbol{r_1}|\boldsymbol{r_t})\,d\boldsymbol{r_1}, \tag{6}$$

where $\mathbf{r}_t$ represents the source point location and it is assumed that $\mathbf{r}_t = (0, z)$ in Section 3. Accordingly, the scattered wave is given as:

$$u_s(\boldsymbol{r}) = \int_S J_H(\boldsymbol{r_2})\frac{\partial G(\boldsymbol{r}|\boldsymbol{r_2})}{\partial n_2}\,d\boldsymbol{r_2}. \tag{7}$$

This can be represented as:

$$u_s(\boldsymbol{r}) = -\int_S d\boldsymbol{r_1}\int_S d\boldsymbol{r_2}\left[\left(\frac{\partial}{\partial n_2}G(\boldsymbol{r}|\boldsymbol{r_2})\right)\times Y_H(\boldsymbol{r_2}|\boldsymbol{r_1})u_{in}(\boldsymbol{r_1}|\boldsymbol{r_t})\right]. \tag{8}$$

Here, Y_H is the operator that transforms incident waves into surface currents on S and depends only on the scattering body. The current generator can be expressed in terms of wave functions that satisfy the Helmholtz equation and the radiation condition. Y_H is well formulated in [12] for H-polarization.

The incident wave is cylindrical and becomes plane approximately around the target because the line source is very far from the target. As a result, we consider $u_{in}(\mathbf{r}_1|\mathbf{r}_t)$ to be represented as:

$$u_{in}(\boldsymbol{r_1}|\boldsymbol{r_t}) = \int_{V_T} G(\boldsymbol{r_1}|\boldsymbol{r}')\times\exp\left[-\left(\frac{kx_1}{kW}\right)^2\right]f(\boldsymbol{r}')d\boldsymbol{r}' = G(\boldsymbol{r_1}|\boldsymbol{r_t})\exp\left[-\left(\frac{kx_1}{kW}\right)^2\right], \tag{9}$$

where W is the beam width. The beam expression is approximately useful only around the cylinder. The average intensity of the backscattering wave for H-wave incidence in turbulence is given by:

$$\langle|u_{sb}(\boldsymbol{r})|^2\rangle = \int_S d\boldsymbol{r_{01}}\int_S d\boldsymbol{r_{02}}\int_S d\boldsymbol{r'}_1\int_S d\boldsymbol{r'}_2 Y_H(\boldsymbol{r_{01}}|\boldsymbol{r'}_1)\,Y_H^*(\boldsymbol{r_{02}}|\boldsymbol{r'}_2)\exp\left[-\left(\frac{kx'_1}{kW}\right)^2\right]\times\exp\left[-\left(\frac{kx'_2}{kW}\right)^2\right]\frac{\partial}{\partial n_{01}}\frac{\partial}{\partial n_{02}}\langle G(\boldsymbol{r}|\boldsymbol{r_{01}})G(\boldsymbol{r}|\boldsymbol{r_{02}})G^*(\boldsymbol{r}|\boldsymbol{r'}_1)G^*(\boldsymbol{r}|\boldsymbol{r'}_2)\rangle. \tag{10}$$

We can obtain the LRCS σ_b using (10):

$$\sigma_b = \langle|u_{sb}(\boldsymbol{r})|^2\rangle\,.\,k(4\pi z)^2\,. \tag{11}$$

We express $|u_{sb0}(\boldsymbol{r})|^2$ in free space as:

$$|u_{sb0}(\boldsymbol{r})|^2 = \int_S d\boldsymbol{r_{01}}\int_S d\boldsymbol{r_{02}}\int_S d\boldsymbol{r'}_1\int_S d\boldsymbol{r'}_2 Y_H(\boldsymbol{r_{01}}|\boldsymbol{r'}_1)\,Y_H^*(\boldsymbol{r_{02}}|\boldsymbol{r'}_2)\exp\left[-\left(\frac{kx'_1}{kW}\right)^2\right]\times\exp\left[-\left(\frac{kx'_2}{kW}\right)^2\right]\frac{\partial}{\partial n_{01}}\frac{\partial}{\partial n_{02}}G_0(\boldsymbol{r}|\boldsymbol{r_{01}})G_0(\boldsymbol{r}|\boldsymbol{r_{02}})G_0^*(\boldsymbol{r}|\boldsymbol{r'}_1)G_0^*(\boldsymbol{r}|\boldsymbol{r'}_2). \tag{12}$$

We can obtain the LRCS σ_{b0} using (12):

$$\sigma_{b0} = |u_{sb0}(\boldsymbol{r})|^2\,.\,k(4\pi z)^2\,. \tag{13}$$

Final forms for (10) and (12) are derived in [16]. To

formulate the fourth moment of the Green's function in these equations, it is needed to use the structure function of turbulence D, defined in [9], as was explained in [13]. It should be noted that equation (3) puts a condition and assumes that the randomness density B is quite low enough to the extent that the medium has a fairly small number of particles resulting in having large separations ρ among particles. In [17], it was proved that D agrees better with the two-dimensional isotropic relation for larger ρ among particles than for smaller ρ. It was concluded that random medium can be considered as a two-dimensional turbulence in the enstrophy inertial range. This was derived and compared with calculations based on wind data from 5754 airplane flights. As a result, three-dimensional problems can be analyzed two-dimensionally under condition (3) in the absence of vortex stretching the nonlinear inertial force in the direction of y-axis of the cylinder that is aligned with the line source. Solving the problem two-dimensionally would in turn reduce greatly the calculation time of the scattered waves intensity in addition to minimizing the memory resources of the computers needed to process the three-dimensional problem that has been pursued in [11].

Let us assume that the coherence of waves is kept almost complete in propagation of a distance $2a$ equal to the mean diameter of the cylinder. This assumption is acceptable in practical cases under condition (3). On the basis of the assumption, it is important here to point out that we are going to present a quantitative discussion for the numerical results in Section 3.

The calculation of scattering data has been restricted to the interval $0.1 \le ka \le 30$. It is quite difficult to exceed this ka limit since greater ka requires a large M which consequently increases the calculation time dramatically.

III. NUMERICAL RESULTS

Although some of the incident wave rays become sufficiently incoherent in the propagation through random medium particles, we should pay attention to the spatial coherence length (SCL) of incident waves around the target. The degree of spatial coherence is defined as:

$$\Gamma(\rho,z)=\frac{\left\langle G(\mathbf{r}_1\,|\,\mathbf{r}_t)G^*(\mathbf{r}_2\,|\,\mathbf{r}_t)\right\rangle}{\left\langle\left|G(\mathbf{r}_0\,|\,\mathbf{r}_t)\right|^2\right\rangle}, \tag{14}$$

where $\mathbf{r}_1 = (\rho, 0)$, $\mathbf{r}_2 = (-\rho, 0)$, $\mathbf{r}_0 = (0, 0)$, and $\mathbf{r}_t = (0, z)$. In the following calculations, we assume $B(\mathbf{r}, \mathbf{r}') = B_0$ and $kB_0L = 3\pi$; therefore the coherence attenuation index α defined as $k^2B_0Ll/4$ given in [9] is $15\pi^2$, $44\pi^2$, and $59\pi^2$ for $kl = 20\pi$, 58π, and 118π, respectively, which means that the incident wave becomes sufficiently incoherent. The SCL is defined as the $2k\rho$ at which $|\Gamma| = e^{-1} \cong 0.37$. In [13], a simplified form of the Γ function in random medium is formulated. Figure 2 shows a relation between SCL and kl in this case and that the SCL is equal to 3, 5.2, and 7.5. We use the SCL to represent one of the random medium effects on the LRCS.

In the following, we conduct numerical results for normalized LRCS (NLRCS), defined as σ_b expressed in (11) to σ_{b0} expressed in (13).

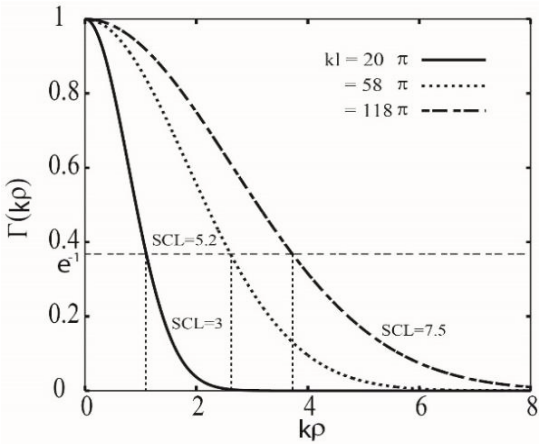

Fig. 2. The degree of spatial coherence of an incident wave about the cylinder.

A. Backscattering enhancement

Airplanes have models where their fuselages have different curvature slopes with the wings. In the numerical results we assume contours of cylinders with different cross section complexities shown in Fig. 3. Intensity of scattered waves varies with the illumination region complexity of such models and the random medium coherence function *SCL*, so we present results in Figs. 4 to 6 showing effects of these cases on the NLRCS. That is, when waves are scattered from fuselage only, we assume that $\delta = 0$ where the cross-section is circular. While waves scattering from other locations in the neighborhood of the fuselage attachment with the wings requires other values for δ such as Q-170 and X-47A airplane ($\delta \cong 0.1$), F16 and F117 airplane ($\delta \cong 0.18$–0.2) [13].

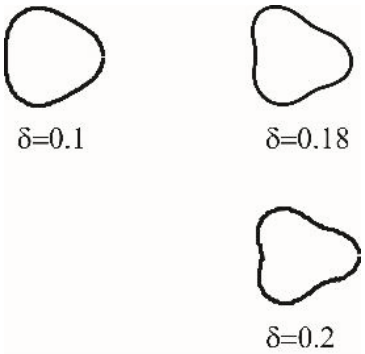

Fig. 3. Contours of cylinders with different cross section complexities.

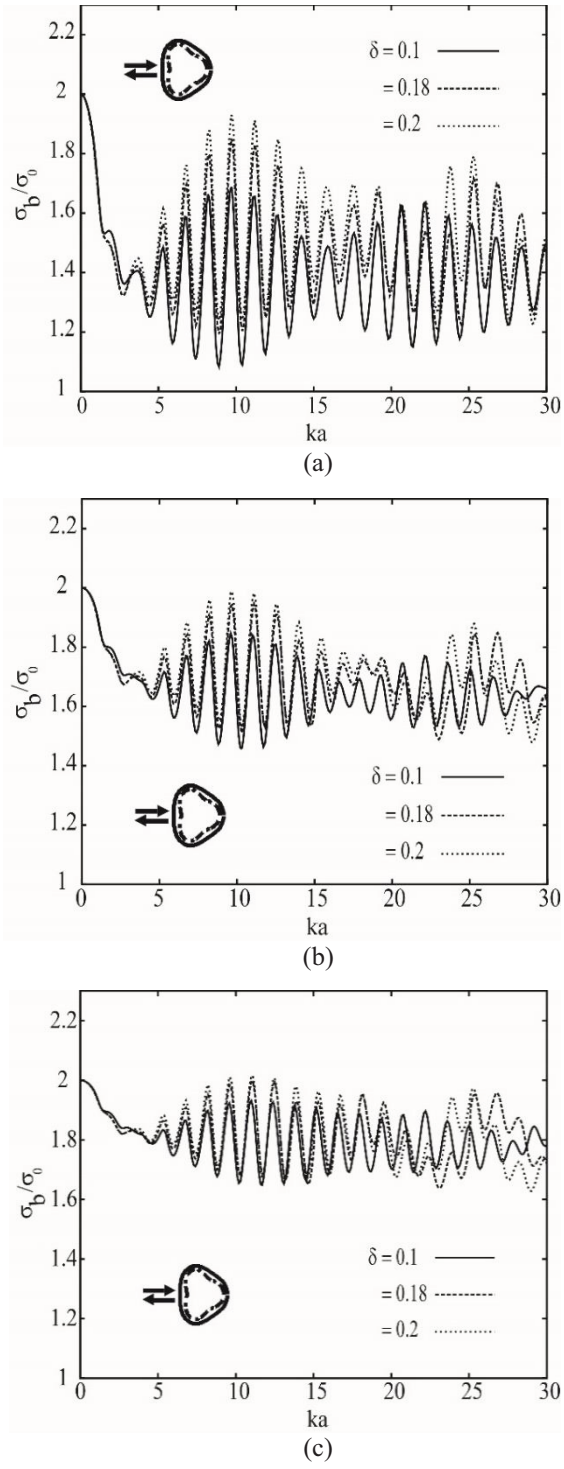

Fig. 4. Normalized LRCS vs. target size at different δ for kW = 2 where: (a) SCL = 3, (b) SCL = 5.2, (c) SCL = 7.5, and σb, σ0 are LRCS in random media and in free space, respectively.

At $ka \cong 0$, NLRCS is two owing to the double passage effect. As ka is getting greater, NLRCS undergoes a substantial oscillating behavior due to the random medium fluctuations. NLRCS is closer to two when having a greater *SCL* which represents a less medium randomness around the object. At the low ka band, target complexity has a less effect on the scattered waves and, therefore, NLRCS is almost invariant and does not change much with different δ. On the other hand, in the high frequency range where $ka \geq 20$, or alternatively at $a \geq 3\lambda$, NLRCS changes relatively more than with the low ka case but yet limitedly with δ. As ka enlarges, as the number of inflection points and accordingly their scattering contributions increase which in turn augments NLRCS. This behavior contradicts with the case of E-wave incidence where NLRCS does not differ with δ within the range $a \geq \lambda$ irrespective of the illumination region [13]. Also, we can notice that, the intensity of the NLRCS fluctuations is greater with H-wave incidence than with the E-wave incidence. This is due to the coupling between the direct waves and the creeping waves. NLRCS have anomaly increases in the resonance region [16] where the mean target size a is close to λ [15]. In addition NLRCS is closer to two with reducing the intensity of the oscillations when the *SCL* is wide enough around the object.

In Fig. 5, we investigate the effect of the illumination region curvature for both concave and convex portions where the incident angle represented in ϕ of Fig. 1 is 0 and π, respectively. It is important to refer to [16], where the illumination region was focused only on the convex portion ($\phi = \pi$) of concave-to-convex objects. It is apparent that the performance of NLRCS with δ discussed above is opposite to its performance with ϕ in Fig. 5. In other words, NLRCS is obviously different with the illumination region curvature at the low ka up to a certain value regardless of the kW limit. That is, NLRCS is different with ϕ at about $a \leq 3\lambda$ and vice versa. In Fig. 6, this observation is valid with *SCL* = 30. While this range is nearly indifferent with kW with the H-wave incidence, the NLRCS performance is, however, different in the case of E-wave incidence where kW would be a factor to determine this certain value of wavelength. This is also attributed to the effect of creeping waves coupling.

From this discussion, we can accept to consider $a \geq 3\lambda$ to be the range where NLRCS would not change obviously with the airplanes dimensions including wingspan and fuselage diameters that can be represented by $2a$ as in Fig. 1. Also within this range, NLRCS can be considered almost invariant with the incident angle, and accordingly with the illumination region complexity, and also with the incident wave polarization. Furthermore, NLRCS avoids having great peaks in the resonance region assuming this range.

As the wingspan is usually greater than the fuselage diameter, then we consider the wingspan to calculate the

proper frequency range for radar system that would reduce and minimizes the error rate of the radar detection system accuracy. Also, it should be noted that the wingspan for civil and military planes are quite different. For example, the wingspan for F16 and X-47A are 10 *m* and 8.465 *m*, respectively, which equals to the diameter 2*a* of the cylinder. As a result, for both models we can accept $\lambda \leq 1.7$ *m* and $\lambda \leq 1.41$ *m* for F16 and X-47A, respectively, and accordingly the frequency can be about 290 MHz or above. For the civil plane, we can consider the Boeing 777 where the wingspan is about 60 *m*. Therefore, $\lambda \leq 10$ *m*, and accordingly the frequency can be about 30 *MHz* or above. Having frequencies above these ranges would reduce the radar error rate and, therefore, maximizes the radar accuracy. As a result, the range of frequencies that can detect the military airplanes can also detect the civil planes, but not necessarily vice versa.

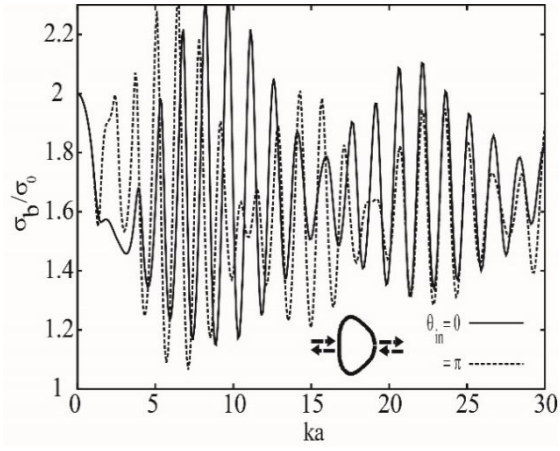

(a)

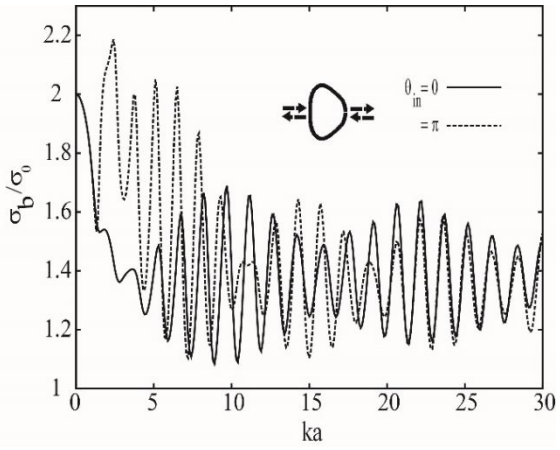

(b)

Fig. 5. Normalized LRCS vs. target size at δ = 0.1 for SCL = 3 where: (a) kW = 1.5, (b) kW = 2, and σb, σ0 are LRCS in random media and in free space, respectively.

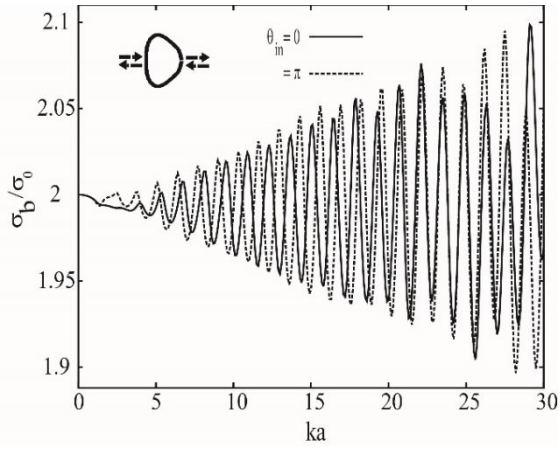

(a)

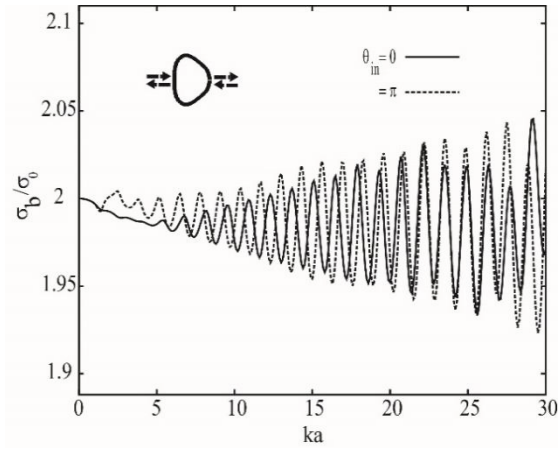

(b)

Fig. 6. As Fig. 5, but for SCL = 30.

IV. CONCLUSION

In this paper, we aim at selecting the range of frequencies that would enhance the capability of radar system to detect airplanes in random medium such as turbulence accurately. In doing this, we investigate the performance of the backscattering enhancement assuming an H-beam wave incidence and compare with the E-beam wave incidence. To maximize the efficiency of a radar system, the normalized laser RCS (NLRCS) should tend to two where the double passage is the only effect for a point target in random medium. This can be achieved with wider SCL and/or wider *kW* and that would also minimize the strength of the peak-to-peak oscillating behavior of NLRCS. On the other hand, NLRCS should be independent of the incident angle and incident wave polarization. Also, the radar frequencies should guarantee that NLRCS avoids having anomaly increases particularly in the resonance region with the convex illumination region.

The range of $a \geq 3\lambda$ can fulfill these requirements,

and hence, the frequencies of 290 *MHz* or above can be used to detect the arbitrary examples of military and civil airplanes assumed in this paper. Higher frequency spectrum minimizes the error rate of the radar system. It should be noted that less frequencies can detect only civil aircrafts but not military ones.

REFERENCES

[1] M. Tropea, F. De Rango, and S. Marano, "Current issues and future trends: DVB-RCS satellite systems," *IEEE A&E Systems Magazine*, pp. 15-22, 2009.

[2] Y. Alvarez, M. Elena De Cos, and F. Las-Heras, "RCS measurement setup for periodic-structure prototype characterization," *IEEE Antennas and Propagation Magazine*, vol. 52, no. 3, pp. 100-106, 2010.

[3] L. Sevgi, Z. Rafiq, and I. Majid, "Radar cross section (RCS) measurements," *IEEE Antennas and Propagation Magazine*, vol. 55, no. 6, pp. 278-291, 2013.

[4] Y. A. Kravtsov and A. I. Saishev, "Effects of double passage of waves in randomly inhomogeneous media," *Sov. Phys. Usp*., vol. 25, pp. 494-508, 1982.

[5] E. Jakeman, "Enhanced backscattering through a deep random phase screen," *J. Opt. Soc. Am*., vol. 5, no. 10, pp. 1638-1648, 1988.

[6] A. Ishimaru, "Backscattering enhancement: from radar cross sections to electron and light localizations to rough surface scattering," *IEEE Antennas and Propagation Magazine*, vol. 33, no. 5, pp. 7-11, 1991.

[7] C. Clemente and J. J. Soraghan, "GNSS-based passive bistatic radar for micro-doppler analysis of helicopter rotor blades," *IEEE Trans. on Aerospace and Electronic Systems*, vol. 50, no. 1, pp. 491-450, 2014.

[8] Z. Q. Meng and M. Tateiba, "Radar cross sections of conducting elliptic cylinders embedded in strong continuous random media," *Waves in Random Media*, vol. 6, pp. 335-345, 1996.

[9] M. Tateiba and Z. Q. Meng, "Wave scattering from conducting bodies in random media−theory and numerical results," *Electromagnetic Scattering by Rough Surfaces and Random Media*, ed. by M. Tateiba and L. Tsang, PIER 14, PMW Pub., Cambridge, MA, USA, pp. 317-361, 1996.

[10] M. Kerker, *The Scattering of Light and Other Electromagnetic Radiation*, Academic Press, New York, 1969.

[11] M. Al Sharkawy and H. El-Ocla, "Electromagnetic scattering from 3D targets in a random medium using finite difference frequency domain," *IEEE Transactions on Antenna and Propagation*, vol. 61, no. 11, pp. 5621-5626, 2013.

[12] H. El-Ocla, "Effect of illumination region of targets on waves scattering in random media with H-polarization," *Waves in Random and Complex Media*, vol. 19, no. 4, pp. 637-653, 2009.

[13] H. El-Ocla and M. Al Sharkawy, "Using CGM and FDFD techniques to investigate the radar detection of 2D airplanes in random media for beam wave incidence," *IEEE Antenna and Propagation Magazine*, vol. 56, no.5, pp. 91-100, 2014.

[14] M. L. Harbold and B. N. Steinberg, "Direct experimental verification of creeping waves," *The Journal of the Acoustical Society of America*, vol. 45, pp. 592-603, 1969.

[15] A. Ishimaru, *Wave Propagation and Scattering in Random Media*, IEEE Press, 1997.

[16] H. El-Ocla, "Influence of incident waves on resonance in backscattering from rargets in random media," *Electromagnetics*, vol. 33, iss. 1, pp. 23-39, 2013.

[17] E. Lindborg, "Can the atmospheric kinetic energy spectrum be explained by two dimensional turbulence?," *Journal of Fluid Mechanics*, vol. 388, pp. 259-288, 1999.

Hosam El-Ocla received the M.Sc. degree in the Electrical Engineering Department of Cairo University in 1996, and the Ph.D. degree from Kyushu University in 2001. He joined the Graduate School of Information Science and Electrical Engineering, Kyushu University, Japan in 1997 as Research Student. He joined Lakehead University in 2001 as an Assistant Professor and has been an Associate Professor since 2007. His current main interests are in wave propagation and scattering in random media.